EXPERIMENTAL STUDY OF WIND LOAD ON TREE USING SCALED FRACTAL TREE MODEL

Conference Paper · June 2019

CITATIONS
0

READS
128

12 authors, including:

Woei-Leong Chan
National University of Singapore
49 PUBLICATIONS **222** CITATIONS
SEE PROFILE

Zhengwei Ge
Institute Of High Performance Computing
25 PUBLICATIONS **84** CITATIONS
SEE PROFILE

Hee JOO Poh
Agency for Science, Technology and Research (A*STAR)
42 PUBLICATIONS **392** CITATIONS
SEE PROFILE

Daniel C. Burcham
National Parks Board
21 PUBLICATIONS **77** CITATIONS
SEE PROFILE

EXPERIMENTAL STUDY OF WIND LOAD ON TREE USING SCALED FRACTAL TREE MODEL

WOEI LEONG CHAN*, YONGDONG CUI, SIDDHARTH SUNIL JADHAV, BOO CHEONG KHOO,

Temasek Laboratories, National University of Singapore, 5A Engineering Drive 1, #09-02, Singapore, 117411

HEOW PUEH LEE

Department of Mechanical Engineering, National University of Singapore, 9 Engineering Drive 1, Block EA #07-08, Singapore, 117575

CHI WAN CALVIN LIM, LIKE GOBEAWAN, DANIEL JOSEPH WISE, ZHENGWEI GE, HEE JOO POH, VENUGOPALAN RAGHAVAN

*Fluid Dynamics Department, Institute of High Performance Computing, Agency for Science, Technology and Research (A*STAR), 1 Fusionopolis Way, #16-16 Connexis, Singapore 138632*

ERVINE SHENGWEI LIN, DANIEL CHRISTOPHER BURCHAM

Centre for Urban Greenery and Ecology (CUGE), National Parks Board, Singapore Botanic Gardens, 1 Cluny Road, Singapore 259569

Green urbanism has stimulated more research on the aerodynamics of tree in recent years. The insight gained in studying wind load on trees would mitigate risk of tree falling and enable sustainable landscape planning. However, deciphering the effect of wind on trees is a daunting task because trees come in various species, shapes, and sizes. In this study, we aim at conducting wind tunnel tests on various species of trees, including measuring the respective drag coefficient and turbulent flow field using a force balance and particle image velocimetry system. The wind tunnel experiment is conducted using scaled down fractal tree model at 10 and 15m/s. The 3D-printed tree model is grown based on the data collected on the species-specific tree parameters, such as the height, trunk diameters, crown box dimensions, etc. In this paper, the wind tunnel result of Yellow Flame (*Peltophorum pterocarpum*) is presented. Results show that the drag coefficient for this inflexible tree model is not sensitive to wind speed. The Reynolds shear stress and turbulence kinetic energy is observed to be the largest at the top and bottom of the crown where the velocity gradients are the highest.

Keywords: Fractal tree model; wind load; Reynolds shear stress; turbulence kinetic energy.

1. Introduction

Experimental study on wind load on trees are usually conducted using real trees in the field [1, 2] or inside large testing facilities [3-6]. Alternatively, scaled down tree models are tested in wind tunnel [7-9] and water tunnel [10-12]. While real trees could yield more realistic results, but the cost is high. On the other hand, the success of scaled down tests lies heavily on the ability to reproduce a scaled down tree model that is accurate to the real trees' physical parameters. We aim to construct species specific scaled down fractal tree model based on real tree data, and conduct wind tunnel test to understand the effect of wind load to the tree

* Corresponding author, Senior Research Scientist, Email: tslcwl@nus.edu.sg.

and the downstream flow field. In this paper, a methodology to construct the tree model and wind tunnel test results of the Yellow Flame (*Peltophorum pterocarpum*) is presented.

2. The Tree Model

In this experiment, the tree model is built as a simple fractal tree based on the estimated[13] height, trunk diameters, and crown box dimensions pertaining to the species found in Singapore. The fractal tree is formed by branches which are each recursively split into 3 child branches for 3 iterations. Figure 1 shows the Yellow Flame tree model. The crown or foliage volume is filled with interconnected elements to form a porous volume. As compared to crown construction using porous material like wool, fibres, and foam as utilized in Ref. 8 and 9, our method allows the average frontal area ratio of dense tropical trees' foliage to be represented accurately. The frontal area ratio is the ratio between the frontal projected areas of the branches and leaves, and the crown shape. The whole tree merged into a single watertight model before sent for selective laser sintering (SLS) printing using polyamide PA2200.

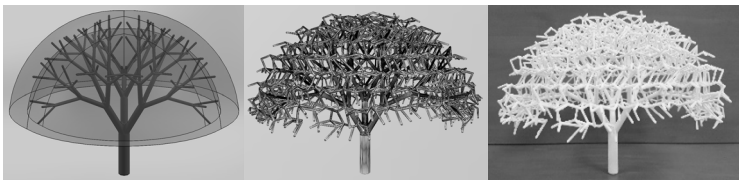

Fig. 1. The computer aided design (CAD) model with defined crown volume (left), the CAD model with porous crown elements (middle), and the 3D-printed model (right) of the Yellow Flame tree.

The dimension of the 1:70 scaled tree model is 260.6 (L) × 259.5 (W) × 176mm (H). Table 1 summarizes other parameters at different rotation angle clockwise about the trunk. Frontal area density (FAD), also known as foliage-element area index in Ref. 14 and 15 is defined as the frontal area of the foliage (leaves and branches) divided by the volume of the crown. It can be interpreted as the reciprocal of the effective depth of the crown.

Table 1. Tree crown frontal projected area and frontal area density

Rotation Angle, deg.	0	30	60
Frontal Projected Area of Foliage (A), m^2	0.016569	0.013264	0.016386
Frontal Area Density, m^{-1}	4.54151	3.63578	4.49151

3. Experimental Setup

The wind tunnel experiment is conducted in a closed-loop low speed wind tunnel with a test section of 0.6 (W) × 0.6 (H) × 2m (L). The tree model is mounted on the ATI Gamma force balance and the force measurement is taken for a duration of 5s at 1000Hz. The particle image velocimetry (PIV) system consists of a Phantom Miro M320s high speed camera, an LDY304 PIV laser, a high speed controller, a laser guiding arm, and laser sheet optics. PIV data is taken at the streamwise centre plane for a duration of 4s at 300Hz.

4. Results and Discussions

4.1. *Drag & Pressure Loss Coefficients*

The drag and pressure loss coefficients are plotted in Fig. 2 and 3. The definition of pressure loss coefficient (λ) is based on the description in Ref. 16 and 17. It is the pressure coefficient loss per unit depth of a porous media. In our case, it can be interpreted as the drag coefficient per unit depth of the tree crown. The coefficients are calculated using the mean force data and the frontal projected area of the crown. The pressure loss coefficient is the product of drag coefficient and FAD.

As observed in Table 2 and Fig. 2, the drag coefficient at rotation angle of 30° is the highest albeit the smallest frontal projected area and slightly lesser drag force. It is likely due to its largest effective depth (smallest FAD). Using the largest streamwise dimension of the crown as an indication to the depth, from 0° to 60° rotation, the respective numbers are 260.6, 272.1, and 257.5mm.

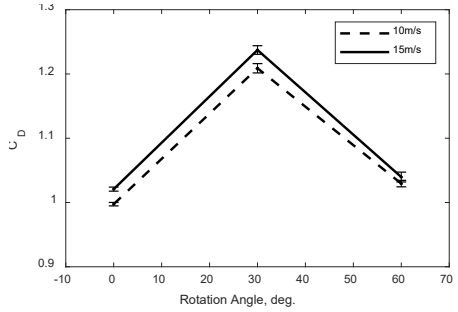

Fig. 2. Drag coefficient at different wind speeds and rotation angles.

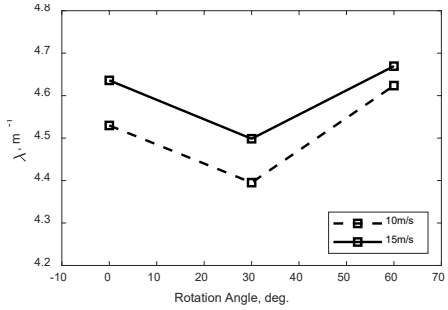

Fig. 3. Pressure loss coefficient at different wind speeds and rotation angles.

Table 2. Drag force and drag coefficient

V_∞, m/s	Rotation, deg.	Mean Drag, N	C_D	V_∞, m/s	Rotation, deg.	Mean Drag, N	C_D
10	0	1.0122	0.9974	15	0	2.3309	1.0208
10	30	0.9821	1.2089	15	30	2.2617	1.2373
10	60	1.0332	1.0294	15	60	2.3477	1.0396

4.2. *PIV Results*

Figure 3 shows the downstream velocity field of 10m/s wind speed. Bleed flow can be clearly seen at the region close to the crown. From the PIV measurement, we extracted the flow field at 1*H* upstream and 2*H* downstream. As shown in Fig. 4, the incoming flow is uniform. The velocity deficit increases from the bottom to the top of the crown with deficit peaks at the top and bottom of the crown, except for the 30° case, which has the least deficit. This is well reflected in the drag force measurement of which the 30° case has the smallest drag. The wake profiles at 10 and 15m/s wind speed are almost identical. This is

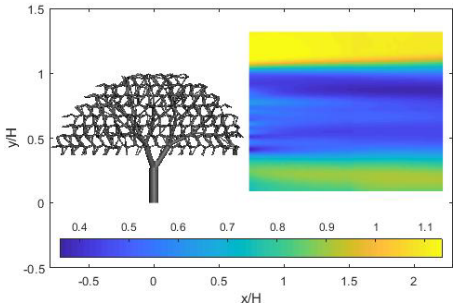

Fig. 3. Downstream velocity field (m/s) at 10m/s free stream wind speed and 0° rotation

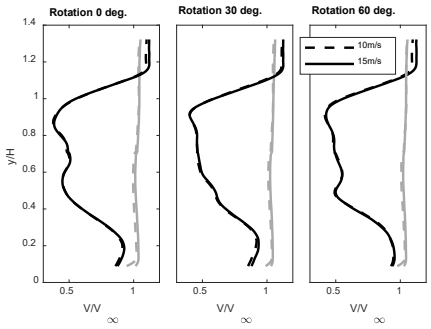

Fig. 4. Normalized wake profile at 1H upstream (grey) and 2H downstream (black)

consistent with the insensitivity of the drag coefficient to wind speed as seen in Fig. 2. Similar insensitivity of inflexible tree models is also mentioned in Ref. 7 and 8.

The normalized mean Reynolds shear stress ($\overline{u'v'}/V_\infty^2$) and normalized turbulence kinetic energy (k/V_∞^2) are plotted in Fig. 5 and 6. It is observed that the flow is highly turbulent at the top and bottom of the crown where the velocity gradients are the highest. Further investigation is needed to correlate these data with the drag force, but the turbulence of the 30° case is notably higher at the top and lower at the bottom.

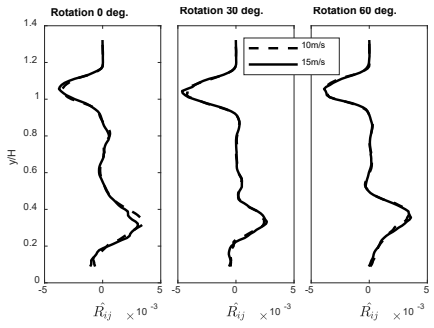

Fig. 5. Normalized mean Reynolds shear stress at 2H downstream.

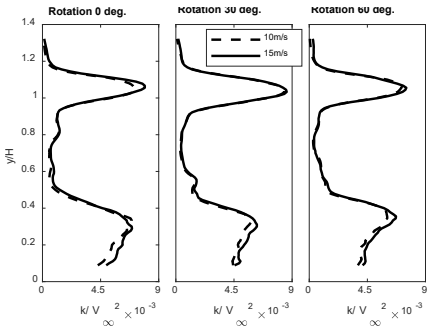

Fig. 6. Normalized turbulence kinetic energy at 2H downstream.

5. Conclusions

A methodology is derived to construct the tree model based on real tree parameters, and wind tunnel tests is conducted to assess the wind load on Yellow Flame tree at 10 and 15m/s wind speed. Study shows that the drag force is insensitive to wind speed and it is dependent to frontal projected area of the crown. However, the drag coefficient shows an inverse correlation to the FAD. Analyses on the normalized mean Reynolds shear stress and turbulence kinetic energy do not yield clear correlation between the drag force and turbulence, but the lowest drag case (with highest FAD and drag coefficient) exhibits higher turbulence on the top of the crown and lower turbulence at the bottom.

Acknowledgments

The authors would like to thank the National Research Foundation of Singapore for the financial support (NRF2017VSG-AT3DCM001-029).

References

1. A. Koizumi, M. Shimuzu, Y. Sasaki and T. Hirai, *J. Wood Sci.* **62** (2016) 363.
2. A. Koizumi, J. Motoyama, K. Sawata, Y. Sasaki and T. Hirai, *J. Wood Sci.* **56** (2010) 189.
3. R. C. Johnson Jr., G. E. Ramey and D. S. O'Hagan, *J. Fluid Eng-T ASME* **105** (1982) 25.
4. M. Rudnicki, S. J. Mitchell and M. D. Novak, *Can. J. For. Res.* **34** (2004) 666.
5. S. Vollsinger, S. J. Mitchell, K. E. Byrne, M. D. Novak and M. Rudnicki, *Can. J. For. Res.* **35** (2005) 1238.
6. J. Cao, Y. Tamura and A. Yoshida, *Urban For. Urban Gree*. **11** (2012) 465.
7. L. Manickathan, T. Defraeye, J. Allegrini, D. Derome and J. Carmeliet, Aerodynamic charaterisation of model vegetation by wind tunnel experiments, *4th Int. Conf. on Countermeasures to Urban Heat Island*, Singapore, 30-31 May and 1 June 2016.
8. C. Gromke and B. Ruck, *Forestry* **81** (2008) 243.
9. R. N. Meroney, *J. Appl. Meteorol.* **7** (1968) 780.
10. K. Bai, C. Meneveau and J. Katz, *Boundary-Layer Meteorol* **143** (2012) 285.
11. K. Bai, J. Katz and C. Meneveau, *Boundary-Layer Meteorol* **155** (2015) 435.
12. K. Bai, C. Meneveau and J. Katz, *Phys. Fluids* **25** (2013) 110810.
13. E. S. Lin, L. S. Teo, A. T. K. Yee and Q. H. Li, Populating large scale virtual city models with 3D trees, *55th IFLA World Congress*, Singapore, 18-21 July 2018.
14. A. S. Thom, *Quart. J. R. Met. Soc.***97** (1971) 414.
15. A. S. Thom, *Quart. J. R. Met. Soc.***98** (1972) 124.
16. C. Gromke, *Environ Pollut* **159** (2011) 2094.
17. C. Gromke and B. Ruck, *Boundary-Layer Meteorol* **144** (2012) 41.